√

CONF-781112--10

MASTER

UCRL-13884

PRIMARY FACTORS GOVERNING HYDRAULIC FRACTURES IN HETEROGENEOUS STRATIFIED POROUS FORMATIONS

M. P. Cleary

August 24, 1978

This paper was prepared for submission to
Energy & Technology Conference of Petroleum Division
Houston, Texas, November 1978

P. O. 8377303

MASSACHUSETTS INSTITUTE OF TECHNOLOGY
CAMBRIDGE, MASSACHUSETTS

eb

DISCLAIMER

PRIMARY FACTORS GOVERNING HYDRAULIC FRACTURES IN HETEROGENEOUS STRATIFIED POROUS FORMATIONS*

by

Michael P. Cleary
Assistant Professor of Mechanical Engineering
Massachusetts Institute of Technology
Cambridge, Massachusetts 02139

ABSTRACT

Some primary material, macrostructural and tectonic features of typical geological formations are identified, insofar as they affect the hydraulic fracturing operation whereby suitably treated fluid is pumped into massive crack(s) underground: the retardation or channeling due to strata interfaces, discontinuities and other heterogeneities is roughly characterised, in the context of fully three-dimensional crack shape evolution, and the initiation from oriented boreholes is discussed in detail. A general-purpose numerical scheme is described, efficiently based on a physically transparent distribution of discontinuity multipoles (or dislocations) and the solution of resulting singular integral equations, which permits precise quantification of these effects: in particular, the barriers provided by adjacent stiffer and tougher strata are properly rationalised and the roles of inelastic slippage, blunting, branching, arrest and re-initiation are placed in more transparent perspective. Stabilisation effects due to alterations of pore-fluid pressure (and hence effective decohering stress), or the flux of formation fluid into the open region near to the crack tip, are described as potentially unfavourable for hydrofrac containment. However, the dominant time-dependent mechanism of frac fluid penetration into the narrow crack aperture attracts most attention: this process is very naturally and tractably incorporated in our comprehensive numerical formulation so that realistic simulation of actual field operations should be feasible in the near future.

NOMENCLATURE

a, b	Minor, major, elliptical crack lengths
A, B	Elasticity parameters, eqn. (6c)
b_F	Blunting amplitude (entrapped dislocation)
c	Diffusivity of porous medium
d	Crack-tip distance from interface
e	Effective radius of elliptical crack
f_s	Friction coefficient on slip surface
E	Elliptic integral (order unity)
E_1', E_2'	Effective moduli of respective strata
E_1, E_2	Principal tensile moduli for anisotropy
g	Ratio of strata shear moduli G_1/G_2
G, G_1, G_2	Shear modulus of each stratum
G, G_{1c}, G_{2c}	Energy release rate, critical values
h	Dislocation distance from interface
J	Path-independent contour integral
K_m	Stress-intensity factors in mode m
ℓ	Generalised crack length
$\underset{\sim}{n}, \underset{\sim}{m}$	Normals to crack surface or perimeter
p, p_T	Fluid pressure in pores, ambient value
p_0	Frac fluid pressure at borehole
$\underset{\sim}{q}$	Flux vector for pore fluid
$\underset{\sim}{Q}$	Frac fluid mass flow vector
r	Distance from borehole or crack-tip
r_1, r_2	Radial co-ordinates from dislocation
r_0, r_{eff}	Radius of borehole, penetration front
t, t_L	Time, lag time from drilling to fracturing
$\underset{\sim}{t}$	Unit vector along crack perimeter
$\underset{\sim}{t}^0$	Traction vector on prospective crack locus
$\underset{\sim}{V}, V$	Frac fluid velocity vector, crack speed
$x_k, y_k; \underset{\sim}{x}$	Cartesian co-ordinates for dislocation;
x, y, z	also for definition of position, stress etc.
α, β	Powers of near-crack-tip singularity
$\Gamma, \Gamma^{(\alpha ij)}$	Elasticity influence functions;
$\Gamma_{(k)}; \Gamma_{jk}^{\ell}$	resulting influence matrix components
δ, Δ	Crack opening displacement, maximum
$\eta, \hat{\eta}$	Viscosity parameters of frac fluid
θ	Position angle in polar co-ordinates
θ_1, θ_2	Polar angles for dislocation
κ	Elasticity parameter $3-4\nu$
μ	Dislocation density (derivative of opening)
ν, ν_1, ν_2	Poisson ratio, of respective strata
τ, τ_L	Dimensionless diffusive time, lag value
ρ	Frac fluid density
$\sigma_{k\ell}$	Cartesian components of stress tensor
$\sigma, \sigma^{(\alpha i)}$	Stresses acting to open or drive fracture
$\sigma_M, \sigma_H, \sigma_V$	Lateral and overburden tectonic stresses
ϕ	Orientation of σ_M to principal direction
ω,	Size of process zone near crack tip,
ω_D, ω_C	for decohesion vs. closure region
$\underset{\sim}{\nabla}^S$	Gradient operator on crack surface

INTRODUCTION

The operation of hydraulically fracturing a formation, from which a valuable resource (e.g. energy, dissolved minerals) may be extracted, has recently been under more intense scrutiny than at any time during its extensive use[1] in the oil and gas industry. Applications to many new areas of endeavor in resource recovery and geophysics are being studied, both experimentally and theoretically: especially, it has gradually been realised that a detailed understanding of the mechanics and materials aspects of the process is essential to reliable design of field equipment and activities. The elementary models previously employed (e.g.) to describe unseen underground response (and even make detailed computations for conditions [illegible] down there, e.g. [7]) must be greatly improved and drastic measures must be taken to escape the current blindness of monitoring equipment.

Some progress has been made toward more realistic estimates for the sequence of events in representative strata and the interaction between the various structural and technological components of particular operations. The determination of *in-situ* stresses (e.g. from "minifrac" tests) has been examined from a more realistic fracture mechanics viewpoint[4], with due consideration[9] of pre-existing flaws, anisotropy, fluid penetration etc. The details of frac fluid flow have been examined more carefully (e.g. in the hot dry rock geothermal context[5]) and computations for its influence have been performed (e.g.[19]). Indeed, the combined effects of frac fluid pressure and tectonic stress distribution have been grossly characterised (e.g.[6]). The question of desirable containment for fractures within specific "pay zone" strata has also been investigated, both experimentally[7] and analytically[8,18]: the observations made are discussed further in this paper. Considerable assistance is available from investigations pursued in other engineering disciplines (e.g. metallurgical and composite material models[10-14]) but there are unique structural and micromechanistic aspects to this rock fracture problem which demand great care in translating conventional ideas of solid mechanics to the current context.

The major goal of this paper is to present an oversight of the factors which can influence the formation and propagation of hydraulic fractures, from the viewpoint of continuum mechanics and the physics of rock deformation mechanisms. Concepts from fracture mechanics are employed, but with emphasis on the character of understanding provided by that discipline rather than on a rigid imposition of code book criteria. Particular attention is paid to the influence, on realistic three-dimensional fracture evolution, of interfaces and discontinuities which are expected to dominate in actual field operations; the potential for arrest, blunting and branching is emphasised and some mnemonic estimates are provided to stimulate more accurate characterisation. We describe a general-purpose numerical scheme which we are using to perform such detailed calculations: this is based on a highly efficient and physically realistic insertion of discontinuity dipoles (or dislocations) to represent tensile cracking, fissure opening, frictional slippage on faults and interfaces and other inelasticity mechanisms which might develop during the main fracture propagation. Besides computational efficiency (e.g. as compared to conventional finite element approaches[21]), the method provides substantial insight into the mechanisms being investigated even without extracting the detailed results, because the representation is so close to physical reality.

Further, our methodology allows for a natural and transparent incorporation of the dominant coupled process whereby fracturing fluid is able to penetrate sufficiently into the elastically opening fracture in order to prop the surfaces apart against confining tectonic stresses and material resistance; again, the form of resulting governing equations facilitates good approximate estimates, even before computer solutions are generated. However, a primary theme is that realistic simulation of typical hydrofracturing operations must unavoidably await the complete numerical implementation of comprehensive analytical formulations which we are now testing: these appear to be sufficiently efficient and physically based, they generate only directly relevant results and they will eventually provide the precise quantification for the mechanisms described heuristically in this paper.

SOME BASIC CONCEPTS FROM FRACTURE MECHANICS

The dominant mechanical features of the hydraulic fracturing process may be most readily extracted with reference to the schematic shown in Fig. 1. Here the actual fractured state at any instant of time (Fig 1(a)) is composed from the stress field pertaining in the absence of any cracking or secondary faulting (Fig. 1(b)) plus a perturbation caused by the need to alter stresses on prospective crack or fault surfaces to their final allowable values (Fig. 1(c)). There may be many such surfaces to be accounted simultaneously (as discussed later in the section on NUMERICAL SIMULATION) but, for clarity, we restrict our description here to the single major fracture which we are attempting to propagate through the strata. The stress distribution in Fig. 1(b) does not make any contribution to the fracture process, since it preserves the continuity of displacements at all points: however, the tractions $\underset{\sim}{t}^{\circ}(\underset{\sim}{x})$ induced on the prospective crack surface (which has unit normal $n(x)$ at any point) will have to be relaxed in accordance with the final fractured state. Thus, the net driving stresses acting to cause the fracture discontinuity and force continued elongation are those shown in Fig. 1(c) namely $pn - t^{\circ}(x)$ applied directly to the crack faces, where $p(x)$ is the fluid pressure induced by the fluid being pumped into the opening fracture: the problem is thereby reduced to a study of the crack locus (appropriately embedded in the surrounding stratified medium), provided we can estimate $t^{\circ}(x)$ from a standard continuum analysis.†

Once we have decided on the driving stresses, our attention must focus on the region around the crack tips where the decohesion is taking place: proper understanding of this process zone requires a rigorous application of both mechanics principles and understanding of material behavior on the microscale. A major simplification in classical fracture mechnaics (valid for many structural applications) has been to lump the materials aspects into a single parameter (e.g.[10]), called the "fracture toughness", expressed either as a 'critical stress intensity factor" K_C or as a "fracture energy" J_C; the former arises from the mathematical deduction that stresses around a crack tip in a linear elastic material have a characteristic singularity (usually $\alpha = +0.5$ in Fig. 1(c) unless the crack-tip is incident upon an interface) while the latter derives from the observation (by Rice[16]) that any effectively elastic material response will result in a path-independent contour integral around a crack-tip, the amplitude of which (J) can be computed by passing the contour along loaded boundaries. Such characterization of the decohesion process by a single amplitude of stress or strain must be applied with great care, especially if macroscopic heterogeneities (surfaces, interfaces, etc.) occur at distances from the crack-tip comparable to the process zone or if the propagation process follows after substantial prior crack growth (as is the case here): indeed, the very events of most interest in hydraulic fracturing (viz., branching, blunting, re-initiation) must necessarily be studied in context of the microstress field and the latter can be deduced from the exterior field (at best characterized by K or J) only after detailed specification of microstructure and processing history.

Nevertheless, the overall capability of driving stresses to induce continued fracture propagation in the crack-tip vicinity can indeed be grossly characterised by quantities that reduce to K or J when the process zone size is much less than any other characteristic dimension for the geometry involved: if done properly, a rough computation of such energy supply amplitudes will always provide a useful (often adequate) first estimate for the study on hand.

†We omit explicit reference to the invariably time-dependent character of these driving stresses, especially of p, [illegible]

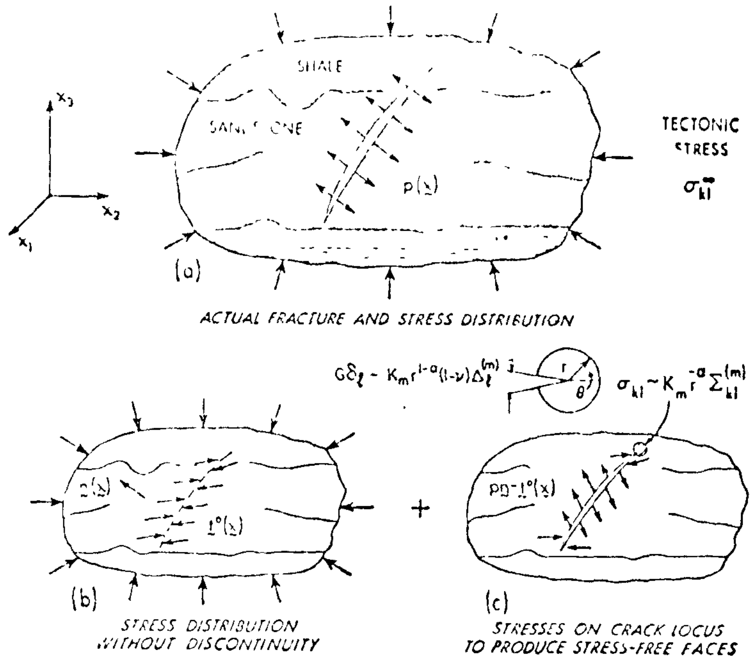

Figure 1. Schematic of superposition process for simulating hydraulic fracture evolution, showing driving stresses and elasticity field around the crack tip.

Thus, it is certainly appropriate to set down the familiar relations of fracture mechanics[10,16] as a starting point for any analysis; in particular, we note the conversion formulae

$$\alpha_1 K_1^2 + \alpha_2 K_2^2 + \alpha_3 K_3^2 = J = G = -dP/d\ell \tag{1a}$$

between stress-intensity factors K_m ($m=1,2,3$ for symmetric tensile, antisymmetric in-plane shearing and antiplane shearing modes, respectively) and the energy release rate $G(=J)$, defined as rate of decrease with crack elongation of total body potential energy P. The coefficients α_m depend on the near-tip elastic anisotropy; for example, we cite the general form of α_1 along with the complete isotropic specialisation.[20]

$$\alpha_1 = -\mathrm{Im}[a_{22}(\zeta_1+\zeta_2)/\zeta_1\zeta_2]/2 \rightarrow (1-\nu)/2G = \alpha_2 = (1-\nu)\alpha_3 \tag{1b}$$

where ζ_1, ζ_2 are the complex roots of the characteristic plane anisotropic equation ($\zeta_1 \rightarrow \zeta_2 \rightarrow i$ for isotropy) and a_{22} is the compliance normal to the crack faces. The appearance of moduli and their potential directionality in these formulae has primary importance in later interpretations, since computations most readily yield K values and a realistic criterion for crack extension will typically be closer to the requirement of a critical J value.

Some straightforward additional modifications of linear homogeneous formulae can now lead to more realistic estimates of crack driving forces. For instance, it will frequently happen (e.g. when material has bilinear stress-strain curve or due to enhanced drainage of pore-fluid at the crack-tip while surroundings remain effectively undrained) that the near-tip material displays one set of moduli while the exterior is governed by a substantially higher stiffness: the net effect is that the more compliant (including decohesion) zone is shielded from the full transmission of the equivalent homogeneous K (and related J) in a manner that can be reasonably accurately represented by the partly mnemonic isotropic expressions,

$$K_e \simeq G_e(1-\nu)K/G(1-\nu_e),\quad J_e \simeq [G_e(1-\nu)/G(1-\nu_e)]^s J \tag{1c}$$

where $s=1,2$ depends on which state (ν,ν_e) is used to compute the reference value J. Estimates like 1(c) can be deduced by matching the discontinuous displacements behind the crack tip (fig. 1(c)). Such logic is also very useful in understanding the behavior of K and J as crack tips approach interfaces between strata of different stiffness (e.g.[10]): if the crack-tip is in the more compliant layer then it is effectively shielded by the stiff adjacent stratum but the contrary applies if it is in the stiffer layer. As well, once the crack has crossed the interface, we may now observe a switch in the condition just described: the stiffer cracked stratum provides more support and the K amplification reverses. Nevertheless, the modulus determining G in eqn. (1a) also undergoes a discontinuous shift and elevation of energy release rate may remain.

On the other hand, it is noteworthy that our computation of K adopts an infinitesimal compliant near-tip zone size (in relation to macro dimensions) but that the process scale may actually be comparable to a critical length (e.g. from crack tip to interface, discussed later): then the assumed locally homogeneity, or even the shielded estimate, must be corrected to account for the further matching of displacements on either side of the constraining boundary (e.g. strata bedding plane) crossed by the process zone. This observation will be seen to remove some formal singularities at interfaces but it obviously has quite practical repercussions. The general character of fracture in heterogeneous media may be qualitatively appreciated by such repeated refinements, but obviously it eventually becomes necessary to perform the detailed numerical calculations described later.

THE ROLE OF INTERFACES AND DISCONTINUITIES

One of the primary questions arising in attempts to successfully fracture an oil- or gas-bearing (e.g., sandstone) formation is whether the crack will be contained in the pay zone or will unavoidably break through to adjacent (e.g. shale) strata and thereby lose effectiveness. There are so many scenarios that we can devise for the events sequential to initial breakdown (discussed later under INITIATION) that only a limited few of the most obvious possibilities can be considered here. For instance, let us assume that an elliptical fracture surface (ACB in Fig. 2(a)) has developed and we are concerned about its further evolution. In particular, we suppose that tectonic stresses (vertical σ_V, horizontal σ_H, and minimum σ_M) dictate the orientation and (despite counteracting frac fluid density) limit the downward spreading (e.g.[6]) so that our major concern is with the competition between upward extension at A as against lateral propagation at C.

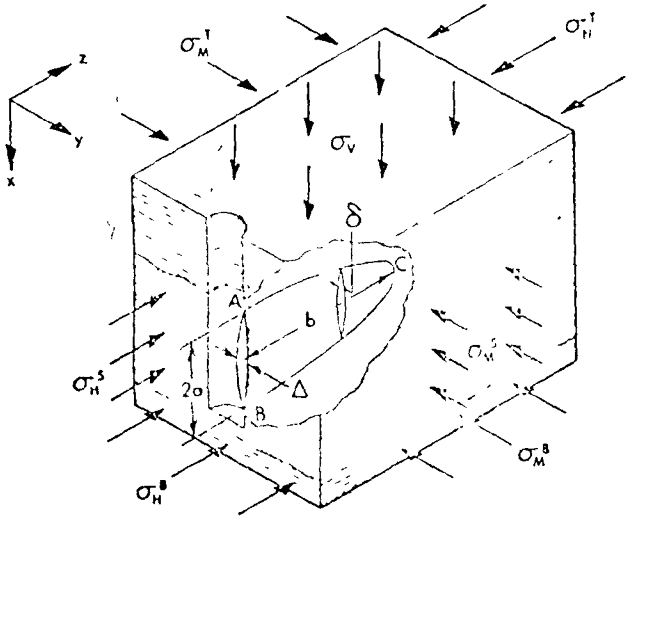

Figure 2.a) Representative geometry and tectonic stresses for vertical hydraulic fracture

Figure 2.b) Geometry of fracture perimeter spreading, elliptical approximation and parameters

$$S \equiv \frac{a b^5 \sqrt{a^2 x^2 + b^2 z^2}}{E\,(a^4 z^2 + b^4 x^2)}$$

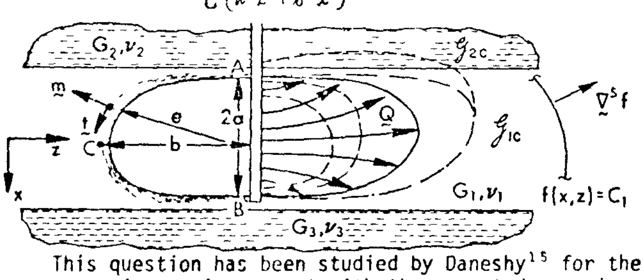

This question has been studied by Daneshy[15] for the homogeneous isotropic context with the expected experimental result that a outstrips b (because of the essentially hyperbolic fluid flow pattern from a line source, as depicted by Q in Fig. 2(b)); if we were to have a horizontal fracture (to which the borehole fluid supply appears as a point source), then the perimeter would spreak outwards as a circle, a behavior to be expected from the vertical fracture only if the process is so slow that effectively uniform pressure is achieved everywhere on the crack faces. Let us take the latter uniform pressure as reference (since it produces optimum conditions for b to exceed a).

Temporarily neglecting local anomalies at the borehole perimeter intersection and the influence of the adjacent heterogeneous strata, we can write an approximate expression for the opening width of the crack,

$$\delta = \Delta[1-(\tfrac{x}{a})^2-(\tfrac{z}{b})^2]^{1/2}, \quad \Delta = 2(p-\sigma_M^S)\,\frac{(1-\nu_1)a}{G_1 E(a/b)} \tag{2a}$$

where $E(a/b)$ is determined from a complete elliptic integral of the second kind (e.g.[17]) but varies from $\pi/2$ (for $a=b$) to unity(for $b\gg a$). An immediate consequence is the expression for stress intensity factor, K, at any point on the perimeter of the crack, provably proportional to the strength of the near-tip singularity in the derivative of opening displacement $\mu \equiv -m.\nabla^s\delta$ (identified later as dislocation or dipole density); using m_x, m_z for component magnitudes of normal vector $\underset{\sim}{m}$ and s for effective radius (Fig. 2(b)), we get

$$[1-(x|a)^2-(z|b)^2]^{1/2}\mu = [m_x(x|a^2)+m_z(z|b^2)]\Delta \tag{2b}$$
$$\doteq 2K(1-\nu)|G\sqrt{\pi s}$$

Immediately, we notice that (for instance) the relevant stress-intensity factors are related by $K_A/K_C \doteq \sqrt{b/a}$, so that any tendency toward non-elliptical shape is countered by stress intensification at the retarded node (assuming presently that K dictates whether the perimeter will extend or not). Thus, it appears that vertical hydraulic fracture propagation in a homogeneous isotropic medium must proceed slowly so as to retain a circular crack perimeter at best; however, the many nonuniformities which can alter this picture, especially the presence of the interface near A, must now be considered.

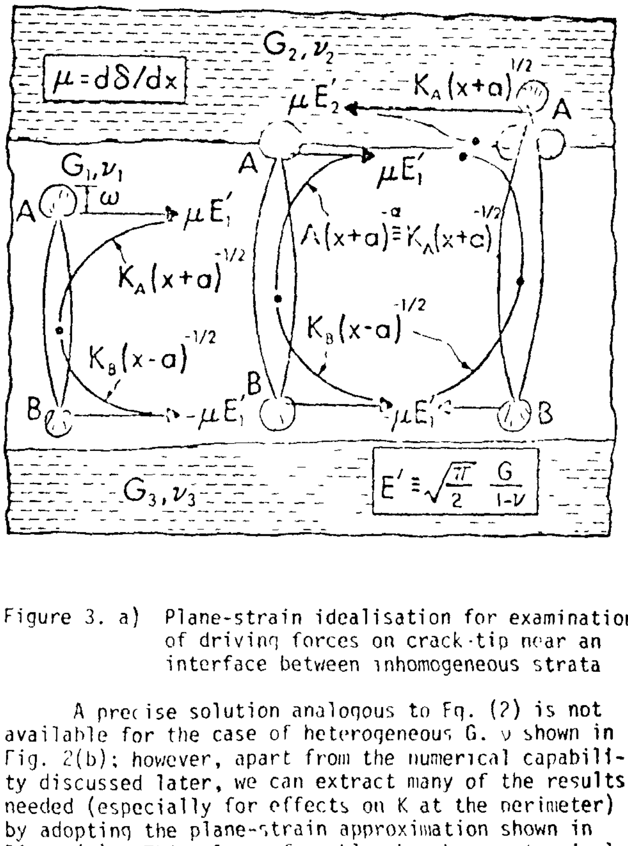

Figure 3. a) Plane-strain idealisation for examination of driving forces on crack-tip near an interface between inhomogeneous strata

A precise solution analogous to Eq. (2) is not available for the case of heterogeneous G, ν shown in Fig. 2(b); however, apart from the numerical capability discussed later, we can extract many of the results needed (especially for effects on K at the perimeter) by adopting the plane-strain approximation shown in Fig. 3(a). This class of problem has been extensively studied by Erdogan and co-workers[10-12,14] and the relevance of their deductions to the hydrofrac situation has been noted previously[8]; still, a substantial amount of further analysis and rationalization is needed here to adequately answer the containment question. Essentially, we examine the behavior of the opening displacement derivative ($\mu = d\delta/dx$) which determines the intensity of stresses around the crack tips (as noted already in Eq. (2)); this presents a square-root singular character (Fig. 3(a)), with amplitude dictated by the stress-intensity factors K_A, K_B unless the tip actually strikes an interface. As the tip approaches very close to such an interface between strata, the character of singularity in μ actually begins to change (to $x^{-\lambda}$, where $\lambda > 0.5$ if the adjacent stratum is softer, while $\lambda < 0.5$ if it is elastically stiffer); for comparison purposes, one may view this behavior as a blow-up or decay of the square-root singularity amplitude K. After the tip passes through the interface, the square-root is restored, so that K returns to finite amplitude, but we note that μ will be discontinuous (even unbounded, with different multiplicative modulus E_2') at points where the crack surface intersects the strata boundary: this means that stresses will be singular at these points, even after crack breakthrough, with potential resulting slip-like decohesion or branching along the interface[17].

A rather simple-minded account of the interface perturbation may be taken by defining the stabilization factors G_H^* and G_S^* (for hard and soft adjacent strata, respectively) as the lowest effective values achieved by the energy release rates by comparison to those pertaining in a homogeneous isotropic medium (Fig. 3(b)). Their identification involves the recognition (either explicitly to remove the arbitrarily low G_H^* or implicitly to provide some stability as the crack crosses into a soft stratum) that the process zone (size ω) will often span the domain (in d/a) of fluctuating K and G: for instance, if the nominal crack tip is having trouble because G_H is dropping severely then the pressure must be built up accordingly and eventually some developing crack in the near-tip decohesion zone will have enough driving energy to link up with the main fracture, thereby producing a new crack with length corresponding to the rising part of the G_H curve. Now we observe that the critical consideration is whether the crack-tip can propagate further into the adjacent stratum at A, as

Figure 3. b) Behavior of stress-intensity factor K and energy release rate $\mathcal{G}$ as crack-tip passes through boundary between different strata

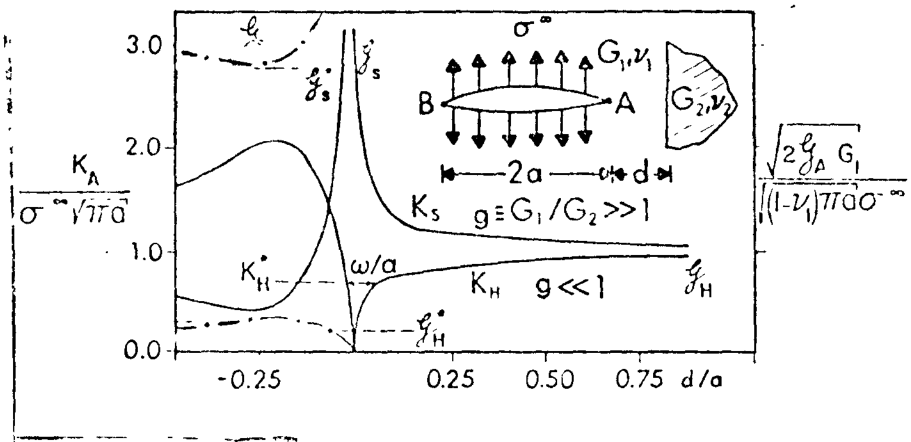

A schematic of the behavior of K_A, for the situation shown in Fig. 3(a) is provided in Fig. 3(b). At first sight, it appears that a stiff upper stratum ($g = G_1/G_2 < 1$) provides an impenetrable barrier while cracks will run unstably into a softer stratum[8] (limited only by the time needed for FRAC FLUID FLOW to reach and pressurize the crack tip region). However, if we carefully examine the details of the response after a crack-tip has passed the interface (temporarily postponing the question of how it gets there) we actually find that the above conclusion is reversed: the amplitude K_A drops ($g>>1$) or rises ($g<<1$) very dramatically with small amounts of extension beyond the boundary (negative d/a in Fig. 3(b)) so that more stability would seem to result from a soft adjacent stratum. [Indeed, it is easy to establish a similar conclusion for the mechanism of blunting and re-initiation at an imperfectly-bonded interface, as we emphasize later]. In actual fact, the most relevant quantity for deciding on propagation facility is probably the energy release rate (eqn. (1b)): if we plot this (fig. 3(b)), we finally realise that the *stiffer adjacent stratum does indeed present the greatest (and persistent) resistance to continued fracturing* (as previously postulated[8]).

The appearance of some dichotomy in our presentation is deliberate since the overall question can be completely resolved only by examing the details of the crack-tip decohesion process itself: the need to do this is reinforced by the recognition that an arbitrarily thin stiffer (but not necessarily tougher) layer would theoretically provide the same perfect barrier to crack propagation in the limit as $d/a \to 0$ and that actual break-through occurs simply because the process zone size (ω in Fig. 3(a)) is not negligible on the scale of characteristic distances in the problem.

against continued expansion at the other extremity C (Fig. 2). If we assign relative toughness G_{1c}, G_{2c} to the respective strata then we can deduce from all of the foregoing, the following rough first estimate for achievable dimensions under very slow fracturing conditions:

$$b/a \doteq G_{2c}/G_{1c}\, G^*(1-K_B^*)^2 \;,\; K_B^* \doteq G b_F/2a^2(1-\nu)\sigma^\infty a \qquad (3)$$

Here we have omitted the potentially unfavorable bias of tectonic stress (vs. hydrostatic frac fluid pressure) distributions[6]; however, more important considerations are the mechanisms of crack blunting and branching which are most likely to favorably retard progress near the interface at A (although they could also be generated by inhomogeneities, faults and fissures near C). To account for these (partly mnemonically) we have inserted a magnitude of blunting b_F (as discussed later under NUMERICAL SIMULATION).

The mechanisms of blunting and reinitiation at interfaces or discontinuities (such as macrofissures, slip faults, etc.) have been given little attention in

+Results in the literature (e.g.[17]) can be misleading in this respect, since they adopt a highly nonuniform pressure on crack faces, designed to preserve a compatibility condition at the interface; such artificiality can be obviated, for instance in use of two cracks with common b_F (eqn.7(d))at the interface. The consistency of results in Fig. 3(b) can be readily appreciated with a simple "strength of materials" argument (matching displacements on either side of the interface) and they appear to be confirmed also by more recent finite element modeling[19].

the study of hydraulic fracturing (or even in more classical applications to materials‡ and structural analysis!), despite their obvious potential for arrest and regeneration in the many complex circumstances which this underground operation may experience. The schematic on left of Fig. 4 illustrates, for the least inhibitive plane strain situation, how simply the crack-tip may lose its nominally sharp contour by onset of slippage along the discontinuity boundary (which may be an interface between strata or just a pre-existing surface with little transverse material bonding): the shear stresses which would be generated near the crack-tip (e.g. see typical element near point B) are too great to be endured by the purely frictional strength corresponding to the normal stresses produced by the combined tectonic conditions and cracking discontinuities. (The latter contribution is negligible only for slippage orthogonal to tensile crack in a homogeneous isotropic medium). The resulting shear-like cracking along the boundary lowers the strength K of the formal stress singularity ahead of the original crack-tip and thus the facility for combined fracture can be reduced substantially. However, there will remain some reduced tensile stress distribution σ_R, with the potential for reinitiation: continued pressurization of the crack faces may elevate this beyond a required critical value, unless the frictional grip across the interface (e.g. represented by coefficient f_s) is too weak, or the adjacent stratum is too elastically compliant. This blunting problem is discussed further under NUMERICAL SIMULATION since very few analytical estimates can be made tractably (and we have inserted K_B^* in Eq. (3) mainly as a mnemonic).

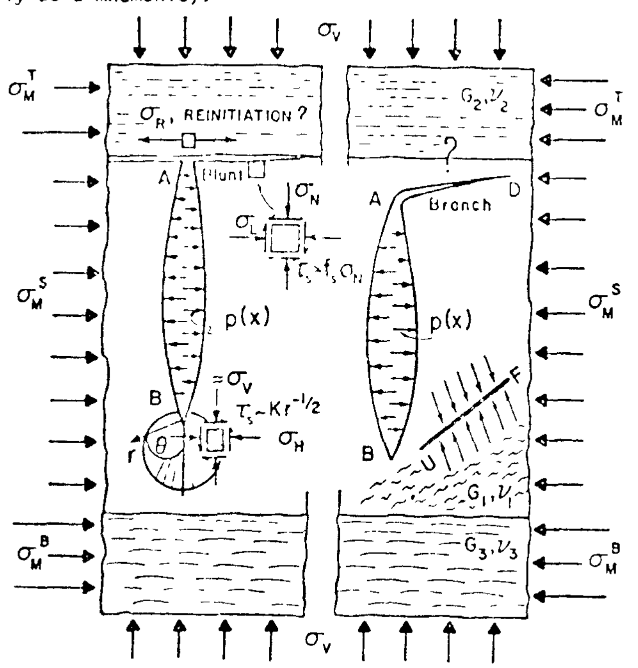

Figure 4. Schematic of mechanisms for partial crack blunting and branching at discontinuity surfaces or in the presence of unfavorable fields ahead

‡Of course, some consideration of finite curvature ("crack-tip opening displacement", slip line fields and near-tip shear-banding) has been included in elastic-plastic fracture analysis (e.g.[16]), but we are concerned further about discrete interaction with local inhomogeneity sites (fissures, bedding etc.)

Crack branching has been subjected to much more scrutiny in the fracture mechanics li ature (e.g.[17]) but the problem is still frequently the object of confusion: a number of continuum criteria (optimum energy release rate, maximum tensile stress, strain energy density) have been proposed to determine when, in a mixed-mode stress field, a crack will branch and in what direction it will go, but little appreciation has been displayed for the dominant role which microstructure and the detailed character of the decohesion process must play in resolving this question. Most obviously, if a pre-existing surface of weakness exists in the macrostructure (e.g. bedding planes or, in the extreme, consider two separate blocks, pressed against each other, being pryed apart) then the fracture will follow that unless it is completely outside the tensile influence (as illustrated by the unfavorable orientation UF in Fig. 4, where compressive stresses remain to keep the fracture closed). On the other hand, the potential for branching may exist in the continuum sense but the required crack path may be very resistant: in essence, we are emphasizing the possible anisotropy and inhomogeneity in cohesive strength even in a reasonably isotropically elastic structure. In addition, however, the scale and character of the process zone always must be considered: none of the damage may be oriented to form a new crack in the favorable direction (viz. microscopic polarization is to be expected) and the decisive local stresses will be highly sensitive to current material state (besides exterior universal stress field). Finally, we note that all theories predict straight-ahead growth under symmetric (mode I) stress conditions but, nevertheless, experiments (e.g.[7,23]) indicate frequent onset of branching as normal cracks approach well-bonded interfaces: one reasonable explanation is that the G_{II} behavior in Fig. 3 is sensed and an alternate lower energy path is found. Again the reliable analysis of branching (especially near interfaces) will involve much more detailed modeling (as discussed under NUMERICAL SIMULATION).

NUMERICAL SIMULATION, GENERAL-PURPOSE COMPUTER PROGRAM

All of the phenomena in foregoing sections (*in-situ* distribution, interface retardation, blunting at discontinuity surfaces, branching to favorable directions, secondary slippage etc.), plus their influence on 3-D evolution of fracture shapes, can be given precise quantitative characterization by means of a comprehensive numerical scheme which we have been developing (e.g. as reported in Ref. 18). To unify the necessarily brief description offered here we provide the most general form of the governing equations being solved, namely

$$u^{(\alpha i)}(x_0, t_0, \mu^{(\gamma k)}) = \sum_{\rho, j} \int_0^{t_0} dt \int_{S_j} dS\, \Gamma^{(\alpha i j)}(x_0, y, t_0, t)\, \mu^{(\rho j)}(x, t) \tag{4}$$

‡This phenomenon is probably suppressed by high confining pressure underground: also, it is facilitated by a bending-type loading which can be present if one end of the fracture has already broken through to a free surface. Indeed, the whole question of fracturability across interfaces[7] can really be tested in the laboratory only when both extremities A & B abut identical adjacent strata, since then the only alternate option is for continued extension at C.

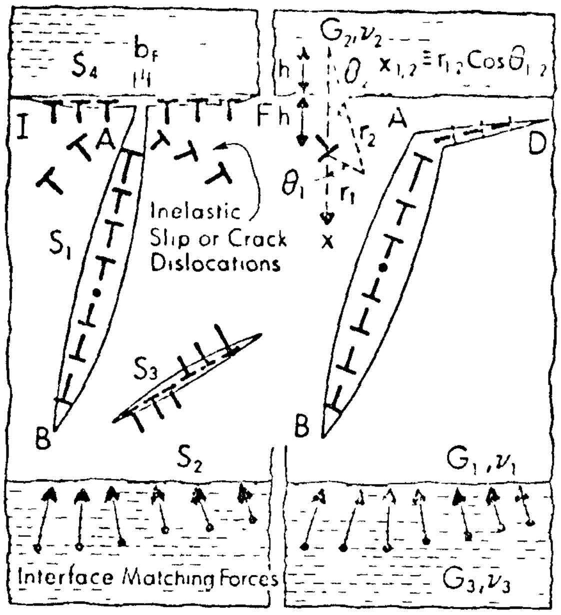

Figure 5. a) Typical combination of fracture events and geometry amenable to numerical analysis (even in 3-D).

The driving stresses $\sigma^{(\alpha i)}$ refer to the α-th component of the traction alteration (for instance $pn - t^0(x)$ in Fig. 1(c)) on the i-th surfaces S_i; they may arise from open cracking (e.g. S_1 in Fig. 5(a)), from frictional sliding on nearby faults (S_3 in Fig. 5(a)), from blunting slippage at the crack intersection with discontinuity surface (S_4) or from the development of a crack branch (S_5). The densities $\mu^{(\beta j)}$ generally represent the corresponding β-th component of displacement discontinuity, on the j-th surface S_j; however, they may also have an interpretation as the distribution of point forces required to patch up conditions across an interface (e.g. S_2 in Fig. 5) which cannot be explicitly incorporated in finding the influence functions for the other surface anomalies. These fundamental solutions[18,20], generically denoted $\Gamma^{(\alpha\beta ij)}$, analogous to the Green's functions for classical potential problems, constitute the α-th traction component at point x_0 on the i-th surface at time t, due to a concentrated density $\mu^{(\beta j)} = \delta(x)H(t)$ at point x; they are derived for a geometry and linear material response as close as possible to that in which the fracture process is being studied. A comprehensive listing of available fundamental solutions is provided in Ref. 18, for both plane strain and fully three-dimensional fracture simulation; further central influence functions are being sought, in particular for a concentrated displacement discontinuity (or dislocation) in a layer between adjacent strata with different moduli (which would remove the need to include S_2 in the numerical scheme, thereby simplifying the task very substantially).

The singular integral equations (4) must usually be solved numerically (except for a few simple analytic solutions with which comparison can be made to verify the programming procedures). Rather than present the most general reduction to matrix algebra (which may be found in Ref. 18), we convey the methodology here with a fairly elementary example (Fig. 5(b)) of a crack oriented normal to an interface between strata. If the pre-existing normal tectonic stress is $\sigma_M(x)$ and the frac fluid pressure distribution is $p(x)$ then Eqns. (4) specialize to

$$\sigma(x_0) \equiv p - \sigma_M = \int_{-a}^{+a} dx\, \Gamma(x_0, x)\mu(x);$$

$$\sigma \equiv \sigma^{(11)},\ \mu \equiv \mu^{(11)},\ \Gamma \equiv \Gamma^{(111)} \tag{5}$$

where $\mu(x)$ is the normal dislocation density (or derivative of opening displacement) and $\Gamma(x_0, x)$ is the normal stress at x_0 induced by an isolated unit dislocation at x.

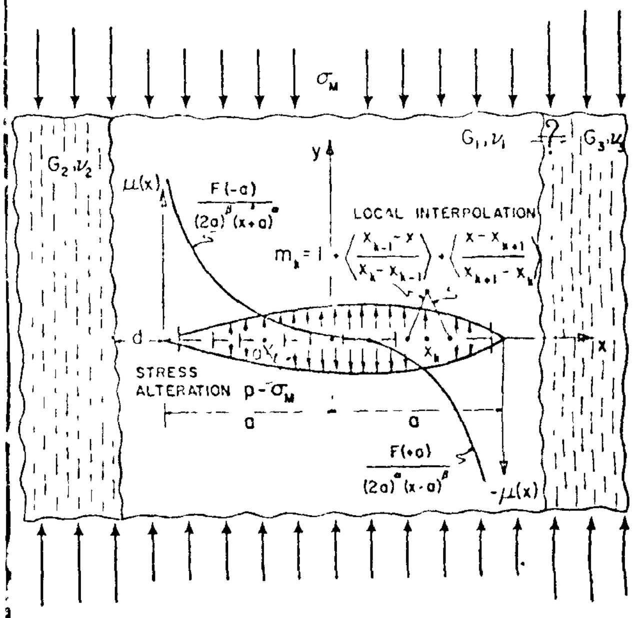

Figure 5. b) Nonuniformly pressurised crack normal to an interface, as elementary illustration of methodology

The latter may be extracted from the very general expression provided in Ref. 18 (deduced for a dislocation near a circular inclusion, using the methodology in Ref. (13)). With reference to the construction shown in Fig. 5(a) we obtain†, for the normal stresses in the respective strata,

$$\begin{Bmatrix} \Gamma_{(1)} \\ \Gamma_{(2)} \end{Bmatrix} = \frac{G_1/\pi}{(\kappa_1+1)} \left[\frac{x_1}{r_1^2} \begin{Bmatrix} 2 \\ 2-A-B \end{Bmatrix} - 2 \begin{Bmatrix} (A+B)x_2/r_2^2 - 2Ah(1-2hx_2/r_2^2)/r_2^2 \\ (A-B)h/r_1^2 \end{Bmatrix} \right] \tag{6a}$$

†We note that $\Gamma_{(1)}$ and $\Gamma_{(2)}$ do not appear to agree with Eqn. (4.4) of Ref. 11 or Eqn. (9) of Ref. 12, each obtained by use of Mellin transform techniques (despite awareness of alternate dislocation technique as employed in Ref. 14); thus, there will be some discrepancies in our final results.

where the relative moduli enter in the following fashion

$$A = (g-1)/(g+\kappa_1), \quad B = (g\kappa_2-\kappa_1)/(g\kappa_2+1); \quad g = G_1/G_2, \quad \kappa = 3-4\nu \tag{6b}$$

We note that $\Gamma(1)$ is singular as $x_1/r_1^2 \sim (x_0-x)^{-1}$, a feature familiar from classical dislocation solutions, but that additional non-singular terms appear to account for the interface.

The discretisation of Eqn. (6a) is now achieved by adopting the following interpolation functions $m_k(x)$ for the dislocation density

$$\sum_{k=1}^{N} a_k m_k(x) \simeq \mu(x) \equiv F(x)/(x+a)^{\alpha}(a-x)^{\beta} ;$$
$$F(x) \simeq \sum_{k=1}^{N} a_k f_k(x) \tag{7a}$$

By imposing Eqn. (6a) at a discrete set of nodal points x_0^j, we now obtain the matrix form

$$(x_0^j) = \sum_{k=1}^{N} \Gamma_{jk} a_k, \quad \Gamma_{jk} = \int_{-a}^{+a} dx\, \Gamma(x_0^j, x) m_k(x) \tag{7b}$$

The explicit extraction of the singular parts $(x+a)^{-\alpha}(a-x)^{-\beta}$ is motivated by their establishment[1-1] as the limiting behavior of $\mu(x)$ when the crack-tips $x=\pm a$ are approached (Fig. 5(b)); further, if the functions $f_k(x)$ are chosen to be the Gauss-Jacobi[22] polynomials, of which special cases are the Gauss-Chebyshev[22] polynomials ($\alpha=\beta=0.5$), then formation of the matrix elements in Eqn. (7b) simply involves the use of standard Gauss-Jacobi integration formulae. Indeed, it is possible to get all the information needed here (e.g. Fig. 3(b)) simply by employing $\alpha \simeq \beta \simeq 0.5$ and allowing the amplitude $F(\pm a)$ to get quite large (without actually letting $d/a \sim 0$): the simplification is apparent in the resulting matrix equations

$$\frac{N}{\pi}\sigma(X_\ell a) = \sum_{n=1}^{N} \Gamma(X_\ell a, t_n a)F(t_n a), \ell = 1,\ldots,N-1 \tag{7c}$$

where t_n, X_ℓ are the zero-points of the Gauss-Chebyshev polynomials, $T_N(t), U_{N-1}(X)$ of the first and second kind, respectively (namely $t_n = \mathrm{Cos}\pi(2n-1)/2N, X_\ell = \mathrm{Cos}\pi\ell/N$). Obviously, an additional condition is needed (to complete the N-1 equations in N variables, Eqn. (7c)) and this takes the form of a "closure criterion"

$$b_F \equiv \int_{-a}^{+a} dx\mu(x) = \int_{-1}^{+1} dX\, F(Xa)/\sqrt{1-X^2} \simeq \frac{\pi}{N}\sum_{n=1}^{N} F(t_n a) \tag{7d}$$

Although this latter condition usually implies merely the simple physical situation where the crack has no "net entrapped dislocation" ($b_F \simeq 0$) there is a great significance for the blunting or branching in Fig. 5(a): there the crack does not close from end to end (regarding AD or IF as a separate crack surface) and b_F must be extracted from the coupling between surfaces. However, the influence of blunting can be examined in a crude way by varying b_F and deducing the effect on stress intensity factors (proportional to $F(\pm a)$) in the numerical scheme: a reference magnitude of this effect has already been cited in Eqn. (3), in the form of K_B^*, estimated for an isolated crack with net entrapped dislocation and numerical solutions are comparing favourably with that estimate.

The solutions of Eqns. (7c,d) produce $F(\pm a)$ and then the stress-intensity factors follow directly (Fig. 3(a)). A corresponding simplicity is not characteristic of other interpolation schemes; we have, nevertheless, been developing alternative *local interpolation functions* m_k (e.g. see Fig. 5(b)) to construct the matrix eqns. (7b): the aim is to preserve greater generality, especially toward problems where the global polynomial schemes are not appropriate. The merit and accuracy of these local approximations (particularly of the piecewise linear "triangular spike" in Fig. 5(b)) has been thoroughly tested (e.g.[20]) and enough detail has been investigated for three-dimensional problems (including efforts with alternate boundary integral formulations[22,23] and some rather special versions[24] of the more general scheme in Eqn. (5)) that we are confident of successful application: particularly, a prime target is the three-dimensional analogue of Fig. 5(b), for which the fundamental solution (point force near boundary of two half-spaces) is already available (Ref. 18).

It is worthy of mention that the various finite element solutions which have been generated (e.g.[22]) can be much more efficiently obtained with a scheme like Eqn. (5); although the finite element method would seem to have greater potential, in the sense of allowing severe local heterogeneity and nonlinearity, it can be quite unwieldy and may even yield somewhat artificial conclusions. In particular, the choice of exterior boundaries (for a necessarily bounded mesh) presents the usual spurious perturbations on solutions in an infinite region; more cogently, however, the character of continuum inelasticity usually assumed in such schemes will typically not be as physically realistic as the discrete slippage events which can naturally be incorporated in the surface discretisation technique described above.

INITIATION, MICROMECHANICS, CONFINEMENT AND PORE-FLUID EFFECTS

Before the hydraulic fracture can get fully established, it must find its way from the borehole to its final massive orientation: wellbore preparation, pumping sequence, stratum heterogeneity or anisotropy and especially microstructural characteristics will play a dominant role in this initiation process. Until recently, however, only a very simple interpretation had been ascribed to the pressure profile $p(t)$, Fig.6, measured in the borehole as the "formation breakdown" develops; for the immediate creation of a vertical fracture, the Timoshenko solution (for a hole in an isotropic homogeneous plate) was applied directly[3], with elementary effective stress modifications for frac fluid seepage into borehole walls, in order to relate p_0 to σ_H and σ_M (Fig. 6). The value of σ_M was then deduced as the "shut-in" pressure after substantial fracture propagation ($\ell \gg r_0$) was deemed to have occurred: little attention was paid to the excess of σ over σ_M, (Fig.6) required to support the fracture at finite interior volume, or indeed to the redistribution and leak-off required to achieve equilibrium. A more sophisticated (equally idealistic) analysis (e.g.[25]) has been popular for quantifying the creation of horizontal hydrofracs: the latter can be typically induced only at very shallow levels in the earth and the complicating perforation process at greater depths still does not prevent them from re-orienting to the vertical (in a direction roughly orthogonal to the mininum principal stress, e.g.[18]).

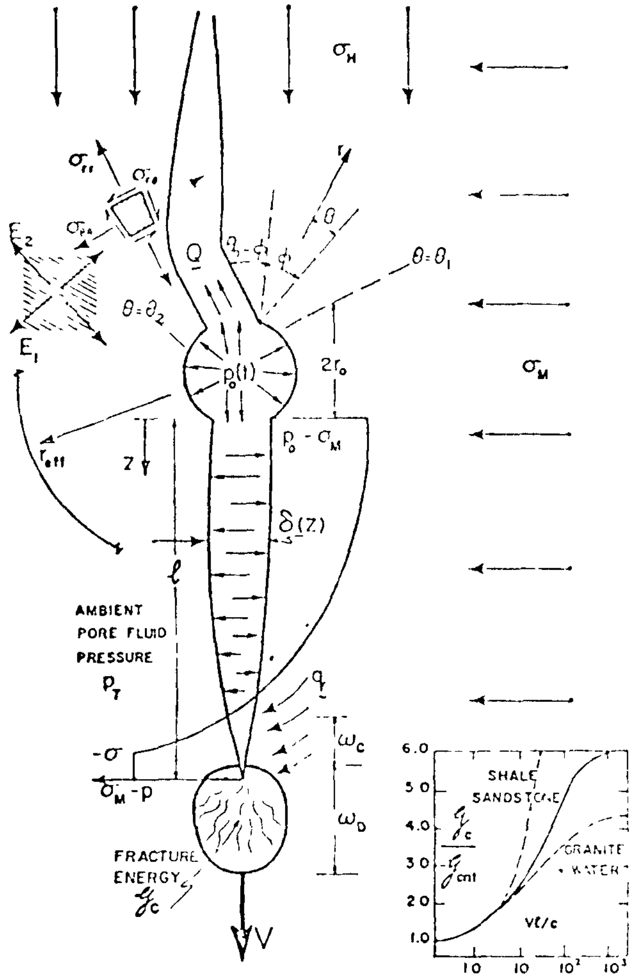

Figure 6. Illustration for initiation from borehole and for effects of confining stresses, formation pore-fluid and frac fluid flow on the evolution of well-established hydraulic fracturing (Inset is curve of "fracture energy" required vs. crack speed, showing strong stabilisation).

§See footnote on next page

Indeed, any fractures which are initially inclined to the most favorable direction (e.g. when borehole is not orthogonal to principal stresses) will tend[26] to curve or branch into their preferred orientation: a proper understanding of the early sequence of events thus requires at least a qualitative appreciation of crack growth in complicated (e.g. mixed-mode) stress fields with due deference to the details of brittle material microstructural response and the role of formation *vs.* frac fluid pressure.

Some elementary but insightful analyses of the early borehole rupture process have more recently been conducted (e.g.[4,9]) and the major conclusions are as follows:

i) Surface flaws, even weak bedding planes (strength anisotropy), major faults or fissures, can easily bias the initiation direction[9] off the superficially favorable orientation ($\theta_0=\phi$, Fig. 6) provided they lie in the zone ($\theta_1<\theta<\theta_2$) of tensile stress induced by the interior pressure (computed in the absence of flaws, since the latter immediately remove the tensile stress on other potential sites); the invariable use of a single tensile strength to characterize onset of rupture (e.g.[3]), even if measured correctly on a representative sample of material (or deduced from re-opening after prior hydrofracturing), thus obviously loses real significance.

ii) Inelastic nonlinearities and realistically severe anisotropy in moduli (e.g. $E_2<<E_1$, Fig. 6) can alter[9] the linear isotropic relation of p_0 to σ_H and σ_M enough to create a 100% error in computing σ_H-σ_M, so that the numerous field measurements of *in-situ* tectonic stresses (e.g.[3]) should at least be accompanied by bounding error estimates.

iii) The pressure required to propagate a near-surface flaw is extremely sensitive to the amount of fluid penetration into cracks and intact borehole walls (plus its interaction with pore-fluid already there), so that the p_0 required to cause rupture will be highly dependent on response characteristics of pumping equipment[9].

iv) Fractures initiated at inclinations to $_H$ may be expected[4] and are experimentally observed[9] to find their way toward the more favorable direction (normal to σ_M) simply because they begin to experience a mixed-mode stress field (e.g.[17]) in which branching is strongly favored energetically; more crudely, it gets increasingly harder to push a fracture out at an angle to σ_H than if it could find its way to normality with σ_M. However, microstructure or strength anisotropy may well dictate its path more strongly than such isotropic energy criteria[17]; indeed, it is not even certain that such an inclined fracture would re-orient as vigorously if it is allowed to close soon enough (and thereby nucleate a shear fault) in a sufficiently compressive tectonic field (a mechanism which we are pursuing as an occasional cheap alternate means of raising formation transmissivity!)

v) Even if multiple fractures can be generated (e.g. by rapid pressurization and suitable casing design) it is very difficult to sustain them: obviously the confining stresses will often favor the closest to σ_H-direction but a competition develops even in an unbiased tectonic field and a pair of cracks out-strip the others[9]. However, it may be possible to exploit the delay time of the FRAC FLUID FLOW penetration and not enough testing has been conducted to eliminate the possibilities for rapid propagation of many cracks (an achievement which would dramatically improve the potential of the technique for many other *in-situ* processing applications).

Among additional features isolated in ref. 9 is the important role that ambient tectonic pore-fluid pressure p_T might play in the pumping sequence required for a successful hydrofrac process. One source of such influence lies in the long time required for pore-pressure around the borehole to equilibrate over distances comparable to desired fracture lengths: this is particularly illustrated by the asymptotic long-time axisymmetric solution of the diffusion equation in cylindrical coordinates which we managed to extract explicitly[5] in ref. 9, namely

$$p \simeq p_T - \pi(p_0 - p_T)Y_0(\hat{r}/\sqrt{\tau \ell n \tau}) \; ; \; \hat{r} = r/r_0, \; \tau = ct/r_0^2 \quad \textbf{(8a)}$$

Here c is diffusivity and Y_0 is the zero-order Bessel function of the second kind: this has the limiting representation $Y_0(z) \to (2/\pi)\ell nz$ as $z \to 0$ and displays an oscillatory behavior for $z \div 0.88$, so that we must limit the domain of relevance to ρ .88 $\sqrt{\tau \ell n \tau}$ in eqn. (8). Beyond this radius, we will have $p \dot{=} p_T$; in particular, we can now express an effective radius in very transparent form (fig. 6)

$$p(r \geq r_{eff}) \simeq (p_o - p_T)/n \;\; \cdot r_{eff} \simeq r_o(\tau \ell n \tau)^{(n-1)/2n} \qquad (8b)$$

This implies that a hydraulic fracture produced at time $t_L \equiv r_0^2 \tau_L / c$ after drilling will experience a strongly-varying pore pressure field at distances $r_{eff} \simeq r_0(\tau_L \ell n \tau_L)^{1/4}$ from the borehole (taking n=2 as reference): typical numbers might be $r_0^2/c \simeq 10$ sec. ($r_0 \simeq 10$cm.), $t_L \simeq 10^7$sec. (4 months) so that $r_{eff} \simeq 50 r_0$, while the full impact of p_T will be felt for $r \gtrsim 2500 r_0$. These distances are well within the range of desired fracture lengths: thus, we must expect a variable intensity of the stabilisation effects (due to formation fluid), discussed next, as the fracture extends to its full length .

The resistance to propagation of a hydraulic fracture obviously has two major sources: the first is the usual need to supply energy (at a rate G_c per unit length of crack advance) for the decohesion process at the crack-tip (zone size ω_D in Fig. 6) but the second is the more dominant closure loading provided by tectonic stress σ_M (in the region where crack opening is too narrow to allow effective frac fluid penetration, size ω_c in Fig. 6). However, even the apparent material constant G_c is strongly affected by the confining stresses σ_H and σ_M; we have[21] found experimentally that σ_H can often decrease the effective toughness (particularly of sedimentary bedded media in the arrester orientation) while an even stronger elevation of G_c with σ_M is being more frequently reported in the rock fracture literature‡. Additionally, we have established[9,20] a dramatic stabilization influence of pore-fluid (inset Fig. 6): if the liquid in the pores has a bulk modulus comparable to the rock matrix (for which we use generic descriptions like granite, sandstone, and shale) then the energy G_c required to propagate a fracture is found to increase dramatically with the speed V (as scaled to c/ℓ, with ω_D/ℓ 0.1 for curves shown in Fig. 6). Even if the pore fluid is a gas, there is an alternate source of crack stabilization: the closure zone ω_c has an effective cohesive stress which rises to σ_M-p, where p is the interior crack pressure in equilibrium with the adjacent formation fluid--thus, p will increase as enough time is allowed for equilibration with ambient† pore-fluid pressure p_T and (in addition to frac fluid pressure redistribution) it will be much easier to propagate the fracture slowly.

§Of course, a complete formal solution is available e.g.[20]) but that defies simple interpretation; we also extracted[9] a solution valid for times $\tau \lesssim 1$ but we realise that this regime is really relevant only to the fluid penetration after p_0 is raised (and must even be modified further if frac and pore fluids do not have comparable viscosities). The lag time (t_L) between drilling and wellbore completion plus fracturing will certainly allow equilibration of pore-pressures induced by σ_H-σ_M, and even the near-borehole gradient in fluid pressure ($t_L \gg r_0^2/c$), but it will not completely eliminate the influence of tectonic pore-pressure gradients.

‡We have previously emphasized[20] the obvious interpretation as a finite zone size $\omega_D \simeq G_c E'/\sigma_T^2$ (σ_T tensile strength) which we find to be of order cms. even for intact rock.

†Obviously, this must be sufficiently compressive also to allow tensile changes of order σ_T ahead of the crack tip (e.g. artesian, deep underground or underwater operations).

DOMINANT INFLUENCE OF FRAC FLUID FLOW

The driving stresses on the main hydraulic fracture ($\sigma^{(1)}$ in Eqns. (5,6a)) are dictated particularly by the degree to which fracturing fluid has been able to penetrate toward the crack-tip and thereby counteract the tectonic confining pressure σ_M. This process requires a suitable flow regime (e.g. of the highly viscous proppant-laden polymeric substance often used); it must be considered in conjunction with the opening induced by deformation of the surrounding stratum since the penetrability of the fracture will be a very strong function of the opening width (e.g.[7]). A typical result for p-σ_M might be the curve shown in Fig. 6 and we can approximate this effectively in various ways (e.g.[20,7]), with resulting estimates to be discussed later; however, the operation is so sensitive to details of that curve (especially near the crack tip) that more accurate numerical solutions are essential. Such modeling has been pursued in recent years (e.g.[19]) but few general conclusions have yet been reached; the fluid flow equations are an essential ingredient in our numerical simulation, so we provide them in the most general form here and then demonstrate the method of simultaneous solution with Eqns. (5,6).

The primary condition is that of mass conservation

$$\underset{\sim}{\nabla}^S \cdot \underset{\sim}{Q} + \partial M/\partial t = -q_L , \quad \underset{\sim}{Q} \;\; \rho\delta \underset{\sim}{V}, \quad M \;\; \rho\delta$$

where ∇^S is the gradient operator in the plane of the crack, Q and M are the fluid mass flow vector and mass content (both integrated across the crack opening) while q_L is the rate of frac-fluid loss to the formation (per unit surface area). The second major criterion is that of momentum conservation

$$-\rho d\underset{\sim}{V}/dt - \langle \underset{\sim}{\nabla}^S \cdot \underset{\sim}{\tau} \rangle + \underset{\sim}{\nabla}^S p \qquad (10)$$

Here $\langle \nabla^S . \tau \rangle$ is the average of the deviatoric stress gradient through the thickness of fluid layer between crack surfaces; it can be deduced from various models of the flow process but an especially simple estimate arises from the Poiseuille-Newtonian velocity distribution (which also happens to have validity for more realistic second order fluids with memory), namely $\langle \nabla^S . \tau \rangle \sim -\hat{\eta} V/\delta^2$, where $\hat{\eta}$ is a suitable constant (depending on geometry).

As an example, consider the situation shown in Fig. 5(b), described by Eqn. (6a); the specialisation of Eqns. (9,10) for the associated one-dimensional flow, is

$$\partial(V\delta)/\partial x = -\partial\delta/\partial t - q_L/\rho \qquad (11a)$$

$$\rho dV/dt = -\frac{\partial p}{\partial x} - \hat{\eta} V/\delta^2, \quad \hat{\eta} = 12\eta \qquad (11b)$$

where η is the dynamic fluid viscosity. Noting that $\mu = \partial\delta/\partial x$ and presently assuming† that $\delta(\pm a) = 0$ (no blunting, etc.), we may integrate Eqn (5) by parts and then perform a partial time derivative: if we then insert eqns. (11a,b) for $\partial\delta/\partial t$ (neglecting loss q_L and inertial terms $\rho dV/dt$) we finally get

$$\hat{\eta} \frac{\partial}{\partial t}[p(x_o) - \sigma_m] \simeq \int_{-a}^{+a} dx \; \Gamma''(x_o, x)\delta^3(x)\frac{\partial p}{\partial x} \qquad (12)$$

where Γ'' is the second derivative of Γ on x. Thus, we

†It is straightforward to incorporate $\delta(-a) = b_F$, Fig. 4, but transparency dictates that we postpone that complication until blunting and linked cracks are under scrutiny.

observe that the increment of fluid pressure distribution at each time can be determined explicitly as the integral of the current solution, provided such a scheme is numerically stable; otherwise, an implicit time-marching scheme is needed, coupling Eqns. (5,12) at each stage. Not enough computing experience is available yet to give criteria for unconditional stability (with the novel equations just presented). Clifton[19] has apparently found implicit marching indispensable for the quite different manner in which he has formulated the coupled equations, namely with δ expressed as an integral over $p(x)$; the above methodology seems to have some distinct advantages, viz. a promise of numerical simplicity, apart altogether from the more readily deducible $\Gamma(x_0,x)$, as against the rather more elusive fundamental solution (for a point-force on the crack face) needed as kernel in his formulation.

It is possible to perform some approximate estimates for the spreading of the crack, as governed by the simultaneous equations in (5) and (12), for instance subject to the condition $\mu\delta'(x=\pm a)\simeq 0$; the latter preserves finite stresses ahead of the tips, almost as if two contacting blocks are being pryed apart since the actual fracture energy will not play an important role in sufficiently rapid propagation. Typical deductions in the past [e.g.[20]] and more recent approximations[9] have taken the form

$$a^{3/2} \simeq C_1[Q^3G/\eta]^{1/4}t + a_0^{3/2}, \quad Q \text{ constant} \tag{13a}$$

$$\ln(a/a_0) \simeq C_2(p_0-\sigma_M)^3 t/G^2\eta\ , \quad p_0 \text{ constant} \tag{13b}$$

where C_1^4, C_2 are constants of order 10^{-1}-10^{-2}. These give an impression of the distinctions between conditions of fixed pumping rate as against constant borehole pressure (for which a more careful estimate of a_0 must be made from the details of initial crack opening due to borehole pressurisation[9]). However, it is misleading to assign other than characterisation value to these (or even to more sophisticated calculations that we have made to approximate the consequences of (5,12)): although fairly simple routines are being used (e.g.[2]) to design actual operations, we believe that accurate solutions (currently being sought for the governing equations described here) are indispensable toward confident predictions with our modelling scheme

SUMMARY AND CONCLUSIONS

In summary, we may list the following primary features which dictate the evolution in extent and shape of a hydraulic fracture.

(1) The fracturing fluid must penetrate into the narrow opening between crack surfaces in order to counteract the tectonic confining pressures and further provide enough decohesion energy for the process zone ahead of the crack perimeter: this requirement strongly favors propagation along the well-bore supplying the fluid (rather than away from it) and even very slow pumping will at best provide a circular crack unless directional material and structure bias appears. In all events, the dominant time-dependence of the operation (e.g. eqn. (10)) will arise from the requirement of adequate FRAC FLUID FLOW.

(2) The presence of interfaces can retard the progress of fractures in a variety of ways (as described mnemonically by eqn. (3)): a) The requirement of elastic compatibility (displacement matching) across the boundary between strata with different moduli causes severe fluctuations in the energy release rate (eqn. (1) and fig. 3) as a fracture perimeter passes through the boundary; the net result can be either strong stabilisation or enhanced propagation (as determined by stress intensity reduction factors K_H^* and K_S^* for "harder" and "softer" adjacent stratum respectively, but with careful account of modulus differences in converting to G, eqn. (1)). As well, b) the interface may be a locus of weak shear bonding - either as a bedding plane between sandstone and shale or as a faulting discontinuity surface, for instance - and the crack tip may partially blunt out by frictional slippage transverse to the propagation direction; we have given a rough characterisation through K_B^* (eqn. (3)) but the breakthrough process may often reduce to a study of re-initiation, for which a stiffer neighbouring stratum is more favorable. c) The proclivity to branching may be heightened by the resistance to propagation experienced at the interface, especially if the crack approaches at an angle to the weak bedding plane; however, laboratory observations of this branching may be suppressed in the field by the confining pressure and absence of a primary fracture breaking through to provide a moment-like effect. d) The relative fractureability of the material in the two strata involved may be completely different: we have characterised these by toughness G_{1c}, G_{2c} (in the usual formal sense of fracture mechanics, eqn. (1)) but there may be a more profound arrest-like retardation in getting a fracture started in the second stratum (because of micromechanism alteration, apart from blunting).

(3) Any favorably oriented weak surfaces (e.g. faults, fissures, bedding planes) may channel the fracture off the otherwise preferred direction; it may arrest as a consequence. Indeed, computations based on isotropy and homogeneity (e.g. for tectonic stresses) may be severely in error because of these.

(4) The fracture may change direction (e.g. branch), especially in a mixed-mode stress field, if it can find a more favorable orientation (either locally or globally). This can cause considerable ambiguity in extracting information from borehole traces (e.g. impression packers), and especially in determining *in-situ* stresses from hydrofrac pressure records, since the well-bore will frequently be inclined to principal stress directions.

(5) Pore-fluid in the stratum being fractured can provide dramatic sources of fracture stabilisation: a) Tensile changes in fluid pressure are induced in the process zone ahead of the crack tip and these temporarily reduce the effective decohesion stress, thereby elevating considerably the energy G_c required for rapid propagation. b) Formation fluid can flow into the zone behind the tip, where frac fluid is barely able to infiltrate and thus increase the very critical pressures on crack surfaces in this vicinity (opposing the tectonic closure stresses). Slow fracturing would require much lower energy release from the driving stresses for such a formation; this could create detrimental influences on fracture shape since we want very slow upward fracturing (by comparison to the desired dominant lateral extension).

(6) Pre-existing tectonic stress inhomogeneities and ansisotropies have the greatest potential to dictate the evolution of fracture shapes: for instance, if the horizontal (minimum) stress increases downward more rapidly than the density-induced frac fluid pressure gradient then upward or lateral extension only will be possible. Large principal stress differences ($\sigma_H-\sigma_M$) help to preserve a consistent fracture orientation, a useful aid in highly variable geological structure at depth. However, field data seem to render unreliable the anticipation that higher lateral stresses in upper (e.g. shale) strata can be exploited to contain hydrofracs in the pay zone.

(7) Anisotropies in material moduli and strengths can substantially alter both the computation of energy rates and the predictions for branching, arrest, blunting etc.

There are, of course, many even more irksome obstacles to a successful hydrofrac job. Maintenance of adequate spacing between fracture surfaces requires careful choice of proppant and great ingenuity in the dispersion process to avoid settlement; besides, subsequent imbedding of the particles in crack walls (especially for high temperature retorting applications) must be prevented, e.g. by use of native crack roughness if some relative sliding can be induced (apparently a feature of a recent success in the geothermal context). Fluid loss to the formation and proper chemical composition (e.g. to prevent weakening reactions) seem to be reasonably manageable features. However, a major stumbling block is the inability to obtain sufficient information from the adjacent underground region before and after operations. Even assuming the required technology is developed to locate geological features, much modelling remains to be done. Efficient and physically based comprehensive numerical schemes, of the kind being developed as indicated in this paper,should serve to alleviate some of those shortcomings.

ACKNOWLEDGMENTS.

The research leading to this paper was supported mainly by the U.S. Department of Energy under contract W7405-ENG-48 (Gas Stimulation Program) to Lawrence Livermore Laboratories, through subcontract with MIT. Additional support came from NSF Grant No. ENG-77-14612 to MIT. I am grateful also for assistance from colleagues at Marathon Oil Company Denver Research Center, since the paper was completed in the early stages of my Industrial Fellowship period (Summer 1978) with that group.

REFERENCES

1. Howard, G.C. and C.R. Fast, Hydraulic Fracturing, Soc. Pet. Eng. Monograph, 1970.
2. Daneshy, A.A., "On the design of vertical hydraulic fractures," Jour. Petroleum Technology, pps. 83-93, 1973.
3. Haimson, B.D., "The state of stress in the earth's crust," Rev. Geophys. Space Physics 13 (3), 350-352, 1975.
4. Abou-Sayed, A.S., Brechtel, C.E., and R.J. Clifton, "*In-situ* stress determination by hydrofracturing-- a fracture mechanics approach," private comm. of Terra-Tek Rep. No. TR 76-36, July 1976.
5. Abe, H., Mura, T., and L.M. Keer, "Growth rate of a penny-shaped crack in hydraulic fracturing of rocks", Jour. Geophys. Res., 81 (29), 5335-5340, 1976.
6. Abou-Sayed, A.S., Jones, A.H., and E.R. Simonson, "On the stimulation of geothermal reservoir by downward hydraulic fracturing," Paper No. 77-Pet-81 presented at ASME Energy Technology Conference and Exhibit, Houston, Sept. 1977.
7. Daneshy, A.A., "Hydraulic fracture propagation in layered formations," Soc. Pet. Eng. Jour., 18, 1, 33-41, 1978.
8. Simonson, E.R., Abou-Sayed, A.S., and R.J. Clifton, "Containment of massive hydraulic fractures," Soc. Pet. Eng. Jour., 18, 1, 27-32.
9. Cleary, M.P., "Some effects of rate and structure in hydraulic fracturing of fluid-saturated porous media," submitted to Jour. Geophys.Research, Dec. 1977.
10. Erdogan, F. (editor), The Mechanics of Fracture, pub. by ASME, 1976 (in particular, see "Fracture of Nonhomogeneous Solids,", pps. 155-170).
11. ... and F. Erdogan, "Stresses in bonded materials with a crack perpendicular to the interface", Int. Jour. Eng. Sci. 10, 677-697, 1972.
12. Erdogan, F. and V. Biricikoglu, "Two bonded half planes with a crack going through the interface," Int. Jour. Eng. Sci. 11, 745-766, 1973.
13. Dundurs, J. and T. Mura, "Interaction between an edge dislocation and a circular inclusion," Jour. Mech. Phys. Solids 12, 177-189, 1964.
14. Erdogan, F. and G.D. Gupta, "The inclusion problem with a crack crossing the boundary", Int. Jour Fracture, 11, 1, 13-27, 1975.
15. Daneshy, A.A., "Three-dimensional propagation of hydraulic fractures extending from open holes", Proc. 15th U.S. Symposium on Rock Mechanics (ed. E.R. Haskins Jr.), pub. by ASCE, pps. 157-179, 1973.
16. Liebowitz, H. (Ed.), Treatise on Fracture , Vol. II, Academic Press, 1968.
17. Gupta, G.D., "Strain energy release rate for mixed mode crack problems", Jour. Pressure Vessel and Piping Technology, ASME Paper No. 76-WA/PVP-7, 1977.
18. Hanson, M.E., Anderson, G.D., Schaffer, R.J., Montan, D.N., Haimson, B., and M.P. Cleary, "LLL Gas Stimulation Program", Quarterly Process Reports No. UCRL 536-78-1,2 from Lawrence Livermore Laboratories, January and April, 1978.
19. Clifton, R.J., "Steady extension of a semi-infinite hydraulic fracture," private communication from Brown University, 1978. (See also Mahmoud, N.O., "On the development of a numerical method for hydrofracturing calculations," M.S. Thesis, Brown University, 1977).
20. Cleary, M.P., "Fundamental solutions for fluid-saturated porous media with applications to localized rupture phenomena,", Ph.D. Thesis, Brown University, 1975.
21. Advani, S.H., Gang Rao, H.V.S., Shuck, L.Z., and H.Y. Chang, "Structural response governing hydraulic fracturing operations in rock media," Final Report from W. Va. University, Morgantown, to ERDA (Contract No. 63-4997), available from NTIS, Nov. 1975.
22. Bui, H.D., "An integral equation method for solving the problem of a plane crack of arbitrary shape", Jour. Mech. Phys. Solids, 25, 29-39, 1977.
23. Cruse, T.A. and F. Rizzo (eds.), Boundary-integral equation methods: computational methods in applied mechanics, , pub. by ASME, 1975.
24. Crouch, S.L., "Analysis of stresses and displacements around underground excavations: an application of the displacement discontinuity method," Univ. Minnesota, Geomech. Report to NSF, Nov. 1975.
25. Kehle, R.O., "The determination of tectonic stresses through analysis of hydraulic well fracturing," Jour. Geophys. Res., 69, 259-273, 1964.
26. Daneshy, A.A., "A study of inclined hydraulic fractures," Soc. Petroleum Eng. Journal, 61-68, April 1973.
27. Tada, H., Paris, P.C., and G.R. Irwin, The Stress Analysis of Cracks , pub. by DEL Research Corp., Hellertown, Pa. 1973.
28. Cleary, M.P., "Some deformation and fracture characteristics of oil shale", pps. 72-82 in Vol. 2 of 19th U.S. Symposium on Rock Mechanics, May 1978.
29. Hanson, M.E., Anderson, G.D., and R.J. Schaffer, "Some theoretical and experimental considerations of the hydraulic fracturing process," verbal description (by M. Hanson) of paper to be presented at Energy and Technology Conference of the Petroleum Division, ASME, Houston, November 1978.

DISTRIBUTION

TID (3)
TIC (2)